Terahertz pulse propagation in a plastic photonic crystal fiber

H. Han,[a] H. Park, M. Cho, and J. Kim
Center for Terahertz Photonics, Pohang University of Science and Technology, San-31 Hyoja-Dong Nam-Gu, Pohang, Kyungbuk 790-784, Korea

(Received 17 July 2001; accepted for publication 12 February 2002)

Guided-wave single-mode propagation of subpicosecond terahertz (THz) pulses in a plastic photonic crystal fiber has been experimentally demonstrated. The plastic photonic crystal fiber is fabricated from high-density polyethylene tubes and filaments. The fabricated fiber exhibits the low loss and relatively low dispersive propagation of THz pulses within the experimental bandwidth of 0.1–3 THz. © *2002 American Institute of Physics.* [DOI: 10.1063/1.1468897]

The recent progress in terahertz (THz) wave generation and detection techniques has generated much interest in low loss THz waveguides which are essential for the construction of compact THz devices and measurement systems. However, most of the present THz systems rely on free space propagation and processing of THz waves due to the virtual absence of low loss waveguides at THz frequencies. The conventional guiding structures such as microstrips, coplanar striplines, and coplanar waveguides fabricated on semiconductor substrates can support only a limited bandwidth due to their excessive dispersion and loss. For example, the power absorption coefficients of coplanar striplines and coplanar waveguides are $\alpha \approx 20\ \mathrm{cm}^{-1}$ at $f=1$ THz, where the frequency dependence on the loss can be expressed as f^r with $r=2-3$.[1,2] Even for micromachined metallic rectangular waveguides, the absorption coefficient is still very high, $\alpha \approx 20\ \mathrm{cm}^{-1}$ at 0.1 THz. Recently, there have been several reports on quasioptical techniques for the efficient and broadband coupling of free space THz radiation into low loss waveguides such as metal, sapphire fiber, and plastic ribbon waveguides.[3–6] The power absorption coefficients of these THz waveguides are found to be less than $1\ \mathrm{cm}^{-1}$ in the THz frequency region.

On the other hand, the photonic crystal fiber (PCF) has engendered growing interest over the past few years since it offers the opportunity to fabricate optical waveguides with enhanced linear and nonlinear optical properties. For example, compared to the conventional optical fibers, the PCF exhibits broadband single-mode operation[7] and air guiding for the reduced nonlinearity and dispersion.[8] A typical PCF consists of a waveguiding core and a spatially periodic cladding region. The core is formed by introducing a defect into the photonic crystal structure to create a localized region with optical properties different from the surrounding cladding region. The guiding mechanism of a PCF depends on whether the effective refractive index of the core is higher or lower than that of the cladding. PCFs with the high index cores guide light by total internal reflection while the waveguiding in ones with the low index cores such as air defects is achieved by the photonic band gap effect.[8]

So far most PCFs have been fabricated from silica due to their applications in optical domain. However, the material loss of silica is prohibitively high at THz frequencies. Thus, for THz applications, low loss materials such as plastics need to be used. The THz applications of these PCFs will depend on the types of the defects. The high-index core PCF can transmit broadband THz signals while the air-core PCF can be used as an ultralowloss, narrow band THz waveguide. In this letter, we experimentally demonstrate the fabrication of a plastic photonic crystal fiber (PPCF) with a high index core. Furthermore, we experimentally show that the fabricated PPCF exhibits low loss single-mode propagation of subpicosecond THz pulses and reasonably low dispersion.

The PPCF was fabricated from 500 μm diameter high-density polyethylene (HDPE) tubes. The HDPE tubes were stacked to form a two-dimensional triangular photonic crystal, and then fused at $\sim 135\,^{\circ}\mathrm{C}$ in a conventional furnace. The lattice constant of the PPCF is 500 μm, and the tube thickness is 50 μm, which corresponds to an air fill factor of 0.673. The total length of the fiber was approximately 2 cm. At the center of the triangular lattice structure, a single solid HDPE filament was inserted to create a high refractive index defect. Shown in Fig. 1 are the optical micrograph of a photonic crystal (a) and the theoretically calculated field distribution of the fundamental guided mode at 1 THz (b). Since the PPCF used in this work has large air holes, it is crucial to use a full vector model for the field calculation.[9] We used the well-known localized mode expansion method using Hermite–Guassian and plane waves.[10,11] It can be seen from Fig. 1(b) that the THz field is highly confined in the defect at 1 THz. Further calculation shows that this field confinement increases as the frequency increases.

The experimental setup for the measurements of THz pulse transmission through the PPCF is similar to that of other THz waveguides measurements.[3–6] It consists of a THz transmitter/receiver and a lens-fiber-lens beam steering/coupling system. The THz pulse was generated via a standard optical rectification method using a (111) semi-insulating GaAs substrate. The generated THz signal is then detected by a photoconductive antenna fabricated on a low-temperature grown GaAs. The PPCF is placed at the THz beam waist between two off-axis parabolic mirrors for efficient coupling in and out of the fiber core. By using a hyper-hemispherical silicon lens, the THz beam is focused to a nearly frequency-independent beam waist of $\sim 500\ \mu$m at

[a]Electronic mail: hhan@postech.ac.kr

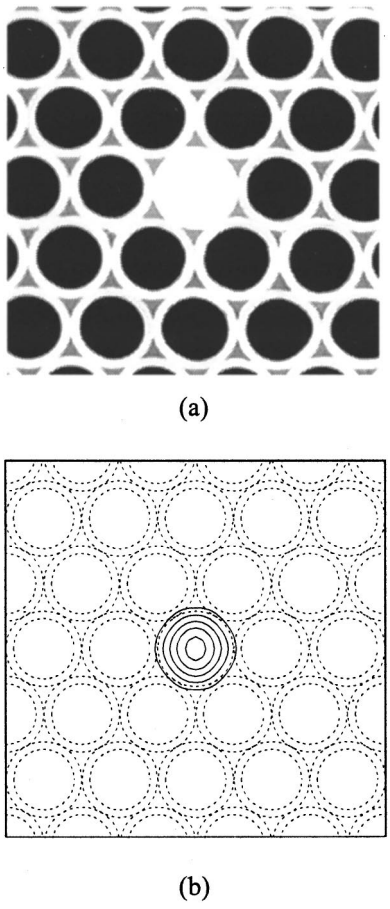

FIG. 1. (a) Optical micrograph of a triangular photonic crystal fiber with a high index defect, and (b) calculated field distribution of a fundamental guided mode at 1 THz.

the entrance face of the PPCF. An identical arrangement is used at the exit face of the PPCF.

A temporal shape of the THz pulse transmitted through the PPCF is shown in Fig. 2, where the inset shows the input pulse measured by removing the PPCF and moving two silicon lenses to back-to-back position, and dotted and solid lines represents experimentally and theoretically obtained results, respectively. The temporal width of the input pulse is measured to be approximately 0.8 ps [full width at half maximum (FWHM)]. As can be seen in the figure the incident

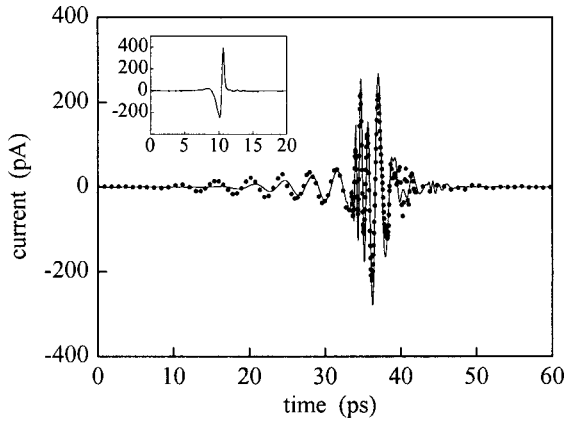

FIG. 2. Measured (dots) and calculated (solid line) pulses after propagating through a 2 cm long plastic photonic crystal fiber. The inset shows the measured input pulse.

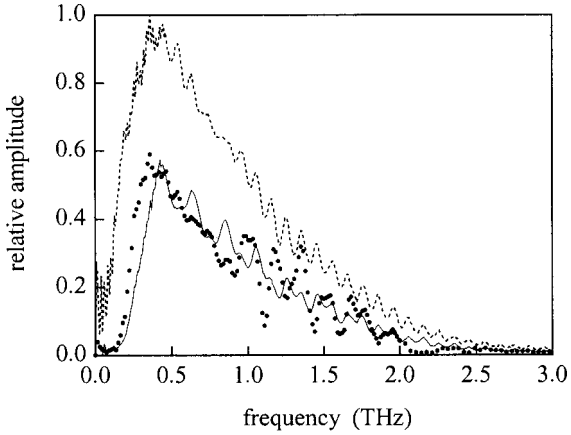

FIG. 3. Amplitude spectra of measured (dots) and calculated (solid line) pulses after propagating through a 2 cm long plastic photonic crystal fiber. The dashed line shows the input pulse spectrum.

THz pulse is chirped to approximately 5 ps (FWHM) after transmission through the PPCF. This corresponds to the average group velocity dispersion (GVD) of approximately 2 ps/THz cm at the center frequency of 0.4 THz. However, a larger GVD can be observed from the highly chirped waves in the lower frequency components at the leading edge of the pulse. This leading part of the transmitted pulse shows normal dispersion whereas the trailing part of the pulse exhibits anomalous dispersion. The observed dispersion is mainly due to the waveguide dispersion in the PPCF. The material dispersion of the HDPE contributed very little to the total dispersion of the PPCF. The theoretical curve (solid line) was obtained assuming the single fundamental guided mode where a frequency-independent refractive index of $n=1.5$. As can be seen in the figure, the theoretical result is in reasonably good agreement with the experiments. The small oscillations after the main peaks (at ~ 40 ps) are due to the interference at the air gap between the PPCF and the silicon lenses.

Shown in Fig. 3 are the amplitude spectra of the THz pulses after propagating through the 2 cm long PPCF, showing that the available spectrum extends from 0.1 to 3 THz where dotted line represents the input wave spectrum, and solid dots and line respresent the measured and calculated transmission spectra, respectively. The small ripples in the transmission spectra are due to the Fabry–Perot effect from the air gap between the PPCF and the silicon lenses. The experimental result shows that the measured spectrum below 0.2 THz is significantly reduced. This is due to the large spatial mode mismatch between the focused Guassian beam and the PPCF guided mode at low frequencies. At 0.2 THz, the effective mode size of the PCF is ~ 3 mm. This is much larger than that of the focused Guassian beam. It is noted that there is no sharp low frequency cutoff for dielectric waveguides such as PCFs with high index defects. The insertion loss of the PPCF including the mode mismatches and the Fresnel reflection losses was measured to be less than 5 dB above 0.4 THz. The upper limit of the power attenuation coefficient of the PPCF was estimated to be less than 0.5 cm^{-1} over the measured spectrum.

The effective and group indices of the PPCF are shown in Fig. 4 as dots and triangles, respectively. The solid and

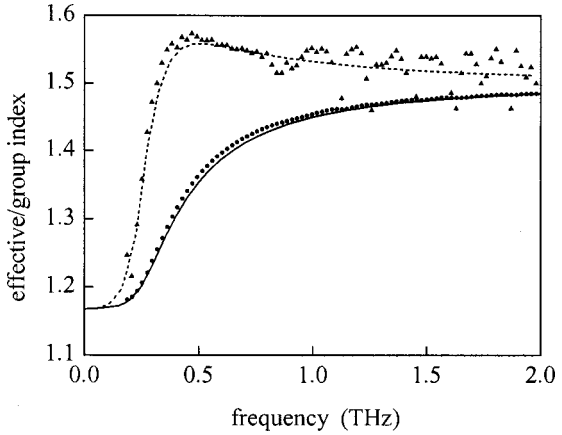

FIG. 4. Effective (dots) and group (triangles) indices. The solid and dashed lines show the theoretical values of effective and group indices, respectively.

dotted lines are the theoretically calculated results for the corresponding experimental data. It is seen that at the high frequency limit, both effective and group indices approach the refractive index of the HDPE core ($n=1.5$) while at the low frequency limit they approach that of the cladding ($n_c=1.163$), the average refractive index of air and HDPE. This is simply because the field confinement in the high index core gets tighter as the frequency increases. In the low frequency part of the spectrum below 0.4 THz, the GVD is large, where the maximum GVD of ~ 14 ps/THz cm occurring around 0.25 THz was deduced from the data. Furthermore, the zero GVD was measured to be around 0.5 THz and the GVD above 0.6 THz was measured to be less than -0.3 ps/THz cm.

The attenuation of a guided mode of the HDPE PCF depends on the field confinement and the material absorption. Based on our measurements and analysis of the data, it is determined that the main contribution of the transmission loss is the material absorption loss. Consequently, the attenuation can be reduced with a better design for lower field confinement in HDPE. Although the HDPE is one of the most widely used materials for lenses and window applications in the THz frequency region due to its transparency, machinability, stability and availability, the published data on the absorption coefficient of the HDPE vary from sample to sample. Depending on the amount of impurities incorporated during the manufacturing processes, the absorption coefficient of the HDPE can be as high as a few cm^{-1}. However, with a certain fabrication method, the HDPE has been shown to have an absorption coefficient as small as $\sim 0.2\ cm^{-1}$ around 1 THz.[12,13] This suggests that the attenuation in the PPCFs can be further reduced by using better HDPE and improved fabrication technique. For narrow band cw THz applications, the absorption-limited attenuation will be minimized in a PPCF with an air core. The fabrication and characterization of an air-core THz PPCF is under way.

In conclusion, we have demonstrated the efficient guided-wave propagation of THz pulses through a PPCF within the bandwidth of 0.1–3 THz. The fabricated PPCF is shown to be low loss and relatively low dispersive where the loss and GVD were measured to be less than $0.5\ cm^{-1}$ and -0.3 ps/THz cm above 0.6 THz, respectively. Such PPCFs have the promise of ultralow loss, mechanically flexible interconnect channels for compact THz devices and systems, especially in frequency-domain investigations with advantages similar to optical fibers.

This work has been supported by the Creative Research Initiatives of the Korean Ministry of Science and Technology.

[1] M. Y. Frankel, S. Gupta, J. A. Valdmanis, and G. A. Mourou, IEEE Trans. Microwave Theory Tech. **39**, 910 (1991).
[2] J.-M. Heiliger, M. Nagel, H. G. Roskos, H. Kurz, F. Schnider, W. Heinrich, R. Hey, and K. Ploog, Appl. Phys. Lett. **70**, 2233 (1997).
[3] R. W. McGown, G. Gallot, and D. Grischkowsky, Opt. Lett. **24**, 1431 (1999).
[4] S. P. Jamison, R. W. McGown, and D. Grischkowsky, Appl. Phys. Lett. **76**, 1987 (2000).
[5] R. Mendis and D. Grischkowsky, J. Appl. Phys. **88**, 4449 (2000).
[6] G. Gallot, S. P. Jamison, R. W. McGowan, and D. Grischkowsky, J. Opt. Soc. Am. B **17**, 851 (2000).
[7] T. A. Birks, J. C. Knight, and P. St. J. Rusell, Opt. Lett. **22**, 961 (1997).
[8] R. F. Cregan, B. J. Mangan, J. C. Knight, T. A. Birks, P. St. J. Rusell, and P. J. Roberts, Science **285**, 1537 (1999).
[9] T. M. Monro, D. J. Richardson, N. G. R. Broderick, and P. J. Bennett, J. Lightwave Technol. **17**, 1093 (1999).
[10] D. Mogilevtsev, T. A. Birks, and P. St. J. Rusell, J. Lightwave Technol. **17**, 2078 (1999).
[11] T. M. Monro, D. J. Richardson, N. G. R. Broderick, and P. J. Bennett, J. Lightwave Technol. **18**, 50 (2000).
[12] *Millimeter and Submillimeter Wave Spectroscopy of Solid*, edited by G. Gruner (Springer, Berlin, 1998).
[13] G. W. Chantry, J. W. Fleming, and P. M. Smith, Chem. Phys. Lett. **10**, 473 (1971).